Stem Cells Translational Medicine, 2024, **13**, 83–99
https://doi.org/10.1093/stcltm/szad073
Advance access publication 3 November 2023
Original Research

Sstr2 Defines the Cone Differentiation-Competent Late-Stage Retinal Progenitor Cells in the Developing Mouse Retina

Yihan Bai[1,2], Han He[1,2], Bangqi Ren[1,2], Jiayun Ren[1,2], Ting Zou[1,2,*], Xi Chen[3,*], Yong Liu[1,2,4,*]

[1]Southwest Hospital/Southwest Eye Hospital, Third Military Medical University (Army Medical University), Chongqing, People's Republic of China
[2]Key Lab of Visual Damage and Regeneration & Restoration of Chongqing, Chongqing, People's Republic of China
[3]Department of Ophthalmology, Beijing Friendship Hospital, Capital Medical University, Beijing, People's Republic of China
[4]Jinfeng Laboratory, Chongqing, China.

[*]Corresponding author: Yong Liu. Email: liuyy99@163.com; or Xi Chen. Email: xichen@ccmu.edu.cn; or, Ting Zou. Email: zoutingcq@163.com

Abstract

Cone cell death is a characteristic shared by various retinal degenerative disorders, such as cone-rod dystrophy, Stargardt disease, achromatopsia, and retinitis pigmentosa. This leads to conditions like color blindness and permanently impaired visual acuity. Stem cell therapy focused on photoreceptor replacement holds promise for addressing these conditions. However, identifying surface markers that aid in enriching retinal progenitor cells (RPCs) capable of differentiating into cones remains a complex task. In this study, we employed single-cell RNA sequencing to scrutinize the transcriptome of developing retinas in C57BL/6J mice. This revealed the distinctive expression of somatostatin receptor 2 (Sstr2), a surface protein, in late-stage RPCs exhibiting the potential for photoreceptor differentiation. In vivo lineage tracing experiments verified that Sstr2$^+$ cells within the late embryonic retina gave rise to cones, amacrine and horizontal cells during the developmental process. Furthermore, Sstr2$^+$ cells that were isolated from the late embryonic mouse retina displayed RPC markers and exhibited the capability to differentiate into cones in vitro. Upon subretinal transplantation into both wild-type and retinal degeneration 10 (rd10) mice, Sstr2$^+$ cells survived and expressed cone-specific markers. This study underscores the ability of Sstr2 to enrich late-stage RPCs primed for cone differentiation to a large extent. It proposes the utility of Sstr2 as a biomarker for RPCs capable of generating cones for transplantation purposes.

Key words: single-cell RNA sequencing; late-stage retinal progenitor cells; cell surface marker; Sstr2; cone differentiation; cell-based therapy.

Received: 3 May 2023; Accepted: 6 October 2023.

Graphical Abstract

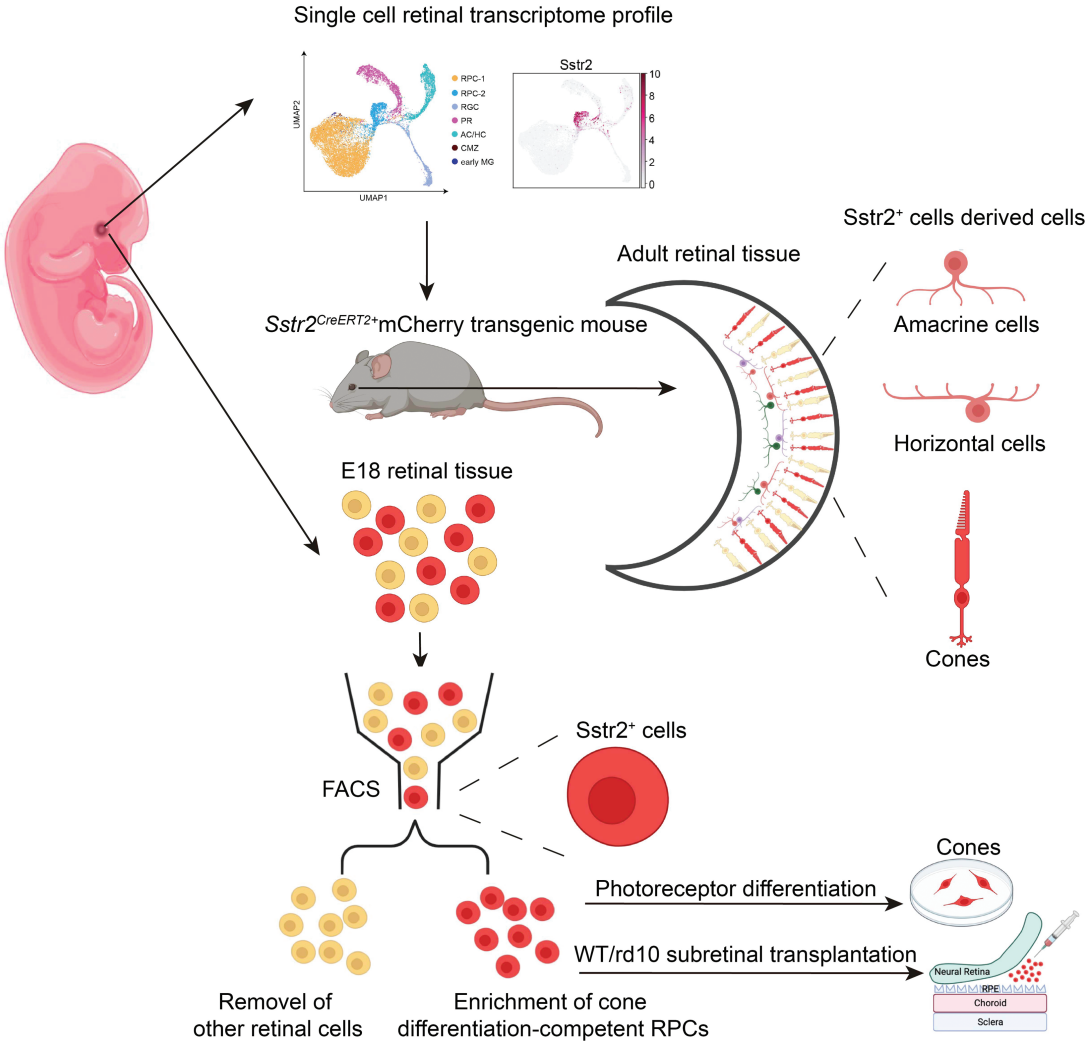

Significance Statement

1. Surface protein, Sstr2, was highly expressed in the late-stage retinal progenitor cell (RPCs) subpopulation with cone differentiation-competency during mouse retinal development.
2. Sstr2$^+$ cells in the late mouse embryonic retinas developed into cones, amacrine cells, and horizontal cells through lineage tracing.
3. Sstr2$^+$ cells expressed RPC markers and differentiated into cones in vitro.
4. Sstr2$^+$ late-stage RPCs subpopulation generated cones in the wide-type and retinal degenerative mice after subretinal transplantation.

Introduction

Retinal degeneration (RD) is a group of disorders that affect the cells in the retina responsible for vision, leading to progressive vision loss over time. The most common form of retinal degeneration is retinitis pigmentosa (RP) and age-related macular degeneration (AMD).[1] Although RD has different causes, the common feature of RD is the gradual loss of photoreceptors, leading to blindness.[2,3] As photoreceptors degenerate, patients with RD often encounter a series of visual impairments. These may include night blindness, tunnel vision, and eventually, a loss of central vision. In certain instances, cone cells, which are responsible for color vision and detailed central vision, can also be affected, resulting in color vision deficiencies and a decline in visual acuity. Despite comprising only 5% of the total photoreceptor population, human cone cells play a crucial role in high-acuity vision, particularly in tasks of daily life that require detailed visual discrimination. The integrity of cone cells is paramount for our ability to perceive color and fine details. Damage to the macula, the region of the retina abundant in cone cells and essential for central vision, can lead to profound and debilitating blindness.[1]

Notably, the photoreceptors that are lost or damaged due to RD have limited capacity for regeneration, and currently, there is no definitive cure for this condition. Stem cell therapy holds significant promise, as transplanted stem cells have the potential to provide support or replace the damaged photoreceptor cells, even in advanced stages of RD.[4] Recently, Ribeiro et al and Gasparini et al generated human iPSC-derived cone lines under the control of L/Mopsin or cone arrestin promoter, respectively; these cone cells can make putative

synaptic connections with host cells and improve photopic light-evoked retinal function and behaviors in the advanced RD mouse model.[5,6] So far, the isolation of RPCs or photoreceptor precursors for transplantation is one of the strategies used to achieve neural retina regeneration.[7,8] However, these cell populations have not yet been adequately identified, partly because of lacking surface markers to label these retinal progenitor cells (RPCs) at different distinct stages. Thus, how to enrich the appropriate donor cells with photoreceptor differentiation potential is a bottleneck for photoreceptor replacement therapy.

Surface marker sorting is a technique commonly employed to identify and isolate specific cell subtypes by utilizing cell surface markers or antigens. This methodology has found significant application in isolating various cell types, including hematopoietic stem cells for clinical bone marrow transplantation.[9] In comparison to isolating cells from genetically modified reporter cell lines or transgenic mouse models, surface marker sorting offers greater ease of operation and is more amenable to clinical implementation. Over the past few decades, numerous surface markers have been identified for the characterization of retinal cells.[10-12] For instance, CD117, also known as c-kit, has been utilized to screen RPCs.[11,13] The c-kit^{+} SSEA4^{-} cells isolated from the human fetal retina and human embryonic stem cells (hESCs) are RPCs with multiple-retinal cell differentiation potential rather than specific photoreceptor differentiation.[13,14] Another maker, CD73, was expressed on the mouse photoreceptor precursors and mature rods and was exclusively expressed in human induced pluripotent stem cells (hiPSCs)-derived photoreceptor precursors.[10,15] Thus, CD73 was applied for purifying photoreceptor precursors and mature rods in the mouse retina and hiPSCs-derived retinal organoids.[15] Another potential biomarker CD133 was also reported to enrich the photoreceptors.[16] However, the effectiveness of CD133 as a marker for late-stage cones in hESC/iPSC-derived retinal organoids is contingent on its interaction with other CD molecules, such as CD26 or CD147.[17] The aforementioned surface proteins can effectively isolate a range of cell types including pan-RPCs, rod-related precursor cells, and late-stage cones, but they do not specifically target pan-cone differentiation-competent RPCs. Discovering suitable surface markers for isolating RPCs or photoreceptor precursors, particularly those with the capability to specifically differentiate into cone cells, holds significant importance for the transplantation-based treatment of RD. In pursuit of this objective, we have identified a novel surface marker, Sstr2, which effectively isolates late-stage RPCs with the potential for cone cell differentiation. Our results introduce a fresh perspective on utilizing Sstr2 as a means to enrich RPCs capable of generating cones, thereby presenting a promising avenue for cell transplantation therapy for RD. This discovery holds the potential to offer a valuable tool for procuring cells aimed at addressing RD.

Methods

Mice

C57BL/6J, *Sstr2*$^{CreERT2+}$, Rosa26-LSL-H2BmCherry, and rd10 mice were raised in the Army Medical University (Third Military Medical University) animal facility, Chongqing, China. The animals were maintained in the standard 12-hour light-dark cycle. All experiments followed the guidelines for the care and use of laboratory animals of Army Medical University (Third Military Medical University) and the ARVO Statement for the Use of Animals in Ophthalmic and Vision Research. All animal experiments procedures complied with the Laboratory Animal Welfare and Ethics Committee of Army Medical University (Third Military Medical University) requirements.

Tissue Dissociation and Preparation of Single-Cell Suspensions

Retina dissociation procedures were performed as described previously.[18] Briefly, eyes were dissected from mice, and retinas were prepared in phosphate-buffered saline (PBS). Eyes from one litter of mice for each sample were used to ensure enough numbers of cells for subsequent analyses. Dissected retinas were then transferred to a dissociation solution containing 6.25 U Papain, incubating for 3 minutes at 37°C. The dissociation was stopped by adding 2% FBS, and then the cells were resuspended in FACS buffer (1× PBS with 1% BSA) with 7-AAD (BD Biosciences, 1 μL /10^{6} cells) for about 5 minutes at 4°C. Cellular aggregates were then removed through a 40 μm filter and sorted using a FACSAria II Flow Cytometer (BD Bioscience). Live cells were selected based on the 7-AAD staining.

Single-Cell Library Construction

Droplet-based scRNA-seq datasets were produced using a Chromium system (10× Genomics, PN120263) following the manufacturer's instructions. Chromium Single Cell 3′ Reagents Kits v2 was used to prepare 10× libraries. Briefly, single cells were partitioned into Gel beads in EMulsion (GEMs) in the GemCode instrument, followed by cell lysis and barcoded reverse transcription of RNA, amplification, shearing, and 5′ adaptor and sample index attachment. The libraries were sequenced on the Illumina Hiseq X Ten platform in a 150 bp pair-ended manner (sequenced by Novogene). Sequencing depth for the E14, E17, and P3 samples were 76 891, 45 509, and 64 411 mean reads per cell, respectively.

Sequencing and Preprocessing Data

Sequencing data from 10× Genomics were aligned and quantified using the CellRanger software package (version 2.1.0) with default parameters. Then, quality control was performed to filter low-quality cells. For mouse retina analysis, only cells with more than 1000 genes and < 3% of their transcripts mapped to mitochondrial genes were retained for downstream analysis. The droplet-based scRNA-seq was expected to generate cell doublets at a low frequency, which could be incorrectly interpreted as distinct cell types. To avoid doublets, cells expressing both Xist and any of Kdm5d, Eif2s3y, Gm29650, Uty, or Ddx3y (genes in the Y chromosome) or identified using doubletdetection (Gayoso and Shor, 2019) were removed in our data. The estimated cell counts for E14, E17, and P3 were: 6123, 9256, and 7185, and 4595, 7234, and 4481 before and after the quality control, respectively.

Dimension Reduction and Clustering

The Seurat (version 2.3.4) implemented in R (version 3.5.0) software was applied for the analysis of E14, E17, and P3 mouse 10×-derived datasets. For E14/E17 data, the UMI count matrix was applied a logarithmic transformation with a scale factor of 10 000. High-variable genes (HVGs)

were calculated using the FindVariableGenes function with parameters "x.low.cutoff" = 0.01,"x.high.cutoff" = 4,"y.cutoff" = 0.45. PCA was performed using HVGs, and significant PCs using the elbow method except for PCs in which most top-ranked genes are related to the cell cycle were selected to perform dimension reduction and clustering. For P3 modified data, the PCA was performed using HVGs with parameter "x.low.cutoff" = 0.125,"x.high.cutoff" = 5,"y.cutoff" = 0.75. Joint analysis of 3 time points of mouse transcriptome data was also conducted by Seaurat and MNN (mutual nearest neighbors, an approach to eliminate batch effects and identify the same cell type across batches[19]). After a single analysis of 3 time points of mouse data, we got their normalized data and HVGs, separately. Then, all the normalized data were put together, and batch effects were mitigated using the mnnCorrect function following the instruction (https://github.com/MarioniLab/MNN2017/blob/master/Droplet/combine_10X.R) with parameters k = 20, subset.row = the combined HVGs from single analysis data. The new data were used as scaled data subjected to Seurat, performing dimension reduction and clustering. Cells were projected in 2D space using UMAP with parameters "n_neighbors" = 20, min_dist = 0.3, and graph-based clustering function Findcluster with parameters "resolution" = 0.6. We also found a cluster that highly expressed *C1qb*, *C1qc*, *Csf1r*, *Fcgr3*, *Itgam* that were enriched in the pathways of leukocyte-mediated immunity, leukocyte migration, cell activation involved immune response in gene ontology analysis. We then excluded this cluster. Finally, 7 discrete clusters were detected and annotated as RPC-1, RPC-2, RGC, PR, AC/HC, CMZ, and early MG.

For further analysis, RPC-2 were subgrouped and reanalyzed by Seurat. For RPC-2, HVGs were selected using the FindVeariableGenes function used for PCA. After evaluating standard deviations of top 50 PCs using PCElbowPlot function, top 5 PCs were selected and imported into FindClusters function (dims.use = 1:5, resolution = 0.3) and tSNE function for dimension reduction and clustering. Three clusters were identified and annotated as Cluster1, Cluster2, and Cluster3.

We performed nonparametric Wilcoxon rank sum tests to find DEGs among different clusters, as implemented in Seurat. DEGs with adjusted *P*-values less than .05 were thought to be significant. We applied the "FindAllMarkers" function with default parameters to identify DEGs, which were then filtered with "logfc.threshold" = 0.5, "min.pct" = 0.25 or 0.15.

Pseudotime Trajectory Analysis

Pseudotime trajectory was constructed with the Monocle 3 package (version 0.1.3) for merged mouse transcriptome data. For merged mouse transcriptome data, after dimensionality reduction and clustering above, we used Monocle3 with function "partitionCells" for partitioning cells into supergroups and function "learnGraph" to organize cells into trajectories based on the concept of "reversed graph embedding." The RPCs of E14 were selected as the roots, and function "plot_cell_trajetory" was used for visualizing the trajectory.

Cell Cycle Analysis

A previously reported core gene set,[20,21] including 43 G1/S and 54 G2/M genes, was used to perform cell cycle analysis using the CellCycleScoring function in Seurat. To reduce the variation in cell cycle status contributing to the heterogeneity in datasets, we performed CellCycleScoring function in Seurat to evaluate the cell cycle status. Then, regressout in ScaleData function removes cell cycle effects before finding HVGs. Besides, we excluded PCs where most top-ranked genes are related to the cell cycle when performing dimension reduction.

Tissue Preparation and Immunofluorescent Staining

For retina tissue immunofluorescence staining, the eyeballs of C57BL/6J, *Sstr2*$^{CreERT2+}$*mCherry*, and rd10 mice were abstracted and then fixed in 4% PFA at 4°C for 2 hours. The eyeballs were successively transferred to 75%, 95%, and 100% ethanol overnight for dehydration. After that, the mice's retinal tissues were embedded in a tissue embedding agent. The samples were cut into slices using a cold microtome and attached to glass slides. Frozen sections of 12-14 μm thickness were immersed in 0.01 M PBS for 3 minutes and repeated 3 times to remove the embedding agent and blocked in 0.01 M PBS containing 10% goat serum, 3% bovine serum albumin (BSA) and 0.5% Triton X-100 at 37°C for 30 minutes. Then the sections were incubated with primary antibodies at 4°C overnight. The next day, removing the primary antibodies solution, the sections were washed with PBS 3 times. Then the sections were incubated with the secondary antibodies at 37°C for 40 minutes. After that, nuclear staining with DAPI for 5 minutes.

For cytoimmunofluorescence staining, the cultured Sstr2$^+$ cells were seeded on cell slides at a concentration of 1.5 × 10^5/mL and fixed in 4% PFA at room temperature for 20 minutes. After removing 4% PFA, the slides of cells were washed with PBS 3 times and 5 minutes each time. Next, the cell samples were blocked in 0.01 M PBS containing 10% goat serum, 3% bovine serum albumin (BSA), and 0.5% Triton X-100 at 37°C for 30 minutes, followed by primary antibodies at 4°C overnight. After washing by PBS 3 times, secondary antibodies were applied to incubate the cell slides at 37°C for 40 minutes, and then nuclear were stained with DAPI.

Both the retina tissue immunofluorescence staining and cytoimmunofluorescence staining were viewed and photographed by a confocal laser scanning microscope (Zeiss, Germany).

The primary antibodies and concentrations used in this study were listed below: rabbit anti-Sstr2 (Abcam, 1:200), rabbit anti-oligodendrocyte transcription factor 2 (Olig2, Abcam, 1:100), rabbit anti-orthodenticle homeobox 2 (Otx2, Abcam, 1:200), rabbit anti-SRY (sex-determining region Y)-box 2 (Sox2, Abcam, 1:200), rabbit anti-cone-rod homeobox (Crx, Atlas antibodies, 1:250), rabbit anti-Arrestin (EMD Millipore, 1:200), rabbit anti-Calretinin (Abcam, 1:200), rabbit anti-M/L-opsin (EMD Millipore, 1:250), rabbit anti-S-opsin (EMD Millipore, 1:250), rabbit anti-transcription factor AP-2, alpha (AP2α, Abcam, 1:200), mouse anti-rhodopsin (Abcam, 1:200), rabbit anti-Calbindin (Abcam, 1:200), mouse anti-protein kinase C alpha (PKCα, Santa Cruz, 1:50), mouse anti-Vimentin (Santa Cruz, 1:50), rabbit anti-Brn3 (Abcam, 1:200). The secondary antibodies were used as follow: goat anti-rabbit IgG Alexa-Fluor-488 (Abcam, 1:500) or goat anti-mouse IgG Alexa-Fluor-488 (Abcam, 1:500) or goat anti-rabbit IgG Alexa-Fluor-647(Abcam, 1:500) or goat anti-mouse IgG Alexa-Fluor-647 (Abcam, 1:500).

Generation of Sstr2 Lineage Tracing Model and Tamoxifen Administration

Sstr2$^{CreERT2+}$ mice, as the lineage tracing model, were generated for the fate-tracking study. Briefly, the Cre-ERT2 construct was inserted into the first exon of Sstr2 to produce *Sstr2*$^{CreERT2+}$ mice. Mice carrying the Sstr2-Cre transgene were identified using Cre-specific primers by PCR analysis of genomic DNA from mice tail samples. Cre recombinase expression was started immediately after the Sstr2 protein began to translate. Without tamoxifen application, the Cre could not enter the nucleus but remained in the cytoplasm. After the induction of tamoxifen, or 4-hydroxy-tamoxifen (4-OHT), the metabolite of tamoxifen, the ERT2 receptor was activated, and Cre was translocated to the nucleus, which promoted recombination. *Sstr2*$^{CreERT2+}$ mice were mated with R26-LSL-H2B-mCherry mice to obtain *Sstr2*$^{CreERT2+}$*mCherry* mice for the lineage tracing model. For Cre activation, tamoxifen was applied. Tamoxifen was entirely dissolved in corn oil (Sigma Aldrich) at a concentration of 20 mg/mL to induce CreERT2 recombination by intragastric administration of 100 mg/kg body weight of tamoxifen (Sigma Aldrich) to pregnant mice at E16.

Isolation and Culture of Mouse Retinal Progenitor Cells

Briefly, the eyes were obtained from E18 embryos from timed pregnant mice, and the eyes were dissected out and rinsed in PBS for once. After removing the cornea, lens, vitreous body, and connective tissues, the remaining retina tissues were cut into small pieces and transferred to the Papain-containing solution (6.25U) incubating at 37°C for 3-5 minutes, afterward adding 2 times the volume of PBS to stop the digestion. The dissociated cells were centrifuged, resuspended with culture medium, and then filtered through a 40-μm filter and seeded in fresh medium containing 1/2 DMEM/F12 and 1/2 Neurobasal supplemented with murine basic fibroblast growth factor (bFGF, 20 ng/mL), murine epidermal growth factor (EGF, 20 ng/mL), N2 (1:100), and B27 (1:50). The approximate yield for RPC isolation was about 8-10 × 10^6 cells per pregnant mouse. The cells were incubated at 37°C 5%CO_2. The culture medium was changed every 2 days.

4-OHT Application and TUNEL Staining

The primary E18 RPCsfrom *Sstr2*$^{CreERT2+}$ mice were inoculated on the 48-well culture plate by 8 × 10^4/well and divided into the 4four different 4-OHT concentration treatment groups: control, 1 μM, 2 μM, and 4 μM, each group with triplicates. After being cultured for 48 hours, the reagent One Step TUNEL Apoptosis Assay Kit (Beyotime Biotechnology) was used for apoptosis detection according to the manufacturer's instructions. In brief, the cells were fixed by 4% paraformaldehyde, permeabilized by 0.5% Triton X-100, and incubated with the mixture of TdT enzyme solution and label solution (1:9) at 37°C for 1 hour. The nuclei of the cells were counterstained with DAPI. The images were viewed and photographed by a confocal laser scanning microscope (Zeiss, Germany). The optimal concentration (2 μM) was applied to induce CreERT2 recombination and activate the expression of Sstr2-mCherry in Sstr2$^+$ RPCs.

FACS of the Mouse Retinal Sstr2-mCherry$^+$ Cells

After being treated with 2 μM 4-OHT for 48 hours to activate the expression of Sstr2-mCherry, the primary retina cells were cultured in a fresh medium for 1 week, the cells were digested with TrypLE Express (Gibco), centrifuged, and resuspended with wash buffer to prepare a single cell suspension. The cell concentration was adjusted to 1 × 10^7/mL after cell counting. The nonviable cells were excluded with cell viability solution (BD Biosciences). Flow cytometry was performed on BD FACS Aria III flow cytometer, and data were analyzed with FlowJo software. The purified cells were used for identifying cell characteristics, differentiation assay, and the following experiments.

Differentiation Characterization Assay

Cell differentiation protocol was performed according to the previous methods with slight modification. The Sstr2$^+$ RPCs were cultured in a medium, which 1/2 DMEM/F12 and 1/2 Neurobasal supplemented with murine basic fibroblast growth factor (bFGF, 20 ng/mL), murine epidermal growth factor (EGF, 20 ng/mL), N2 (1:100), and B27 (1:50) after flow cytometry for the first 48 hours. And then the cells switched to photoreceptor differentiation medium, which included taurine (50 μM; Sigma-Aldrich), retinoic acid (1 μM; Sigma-Aldrich), γ-secretase inhibitor (DAPT, 10 μM; MedChemExpress, MCE), and 1% FBS, and cultured for 14 days. The culture medium was changed every 2 days.

Subretinal Transplantation

According to the protocol for subretinal transplantation,[18] all animals began to receive drinking water containing cyclosporine A (0.2 mg/mL) from 48 hours before transplantation to post-transplantation 2 weeks. Sstr2$^+$ cells were digested with TrypLE Express (Gibco) and resuspended in HBSS supplemented with 0.005% DNase I to prepare cell suspension for transplantation. The wild-type or rd10 mice at P14 were anesthetized with 0.5% pentobarbital sodium. Next, atropine and surface anesthesia were applied to the eye surface. A cut was made on the temporal sclera; then the cells were injected slowly into the subretinal space by a 33-gauge Hamilton needle (Hamilton). For each eye, 1 μL cell suspension containing 1 × 10^5 cells was injected.

Quantitative Analysis

For the distribution analysis of mCherry$^+$ cells in the retina, 3 eyes were included to make slices, and for each section, 3 (400×) visual fields were taken for imaging. For the quantitative analysis of TUNEL$^+$ cells, 2 cell slides were included from each experimental batch of each group, and the experiment was independently conducted 3 times. For the quantitative analysis of Sstr2$^+$ cells and Sstr2$^-$ cells expressed RPC markers and photoreceptor precursor markers, 2 cell slides were included from each experimental batch of each group, and the experiment was independently conducted 3 times. Three (200×) visual fields of the cell slide were taken. Images of the retina slices or cell slides were taken under a Zeiss confocal microscope, and the data were measured by ImageJ (NIH, USA).

Statistical Analyses

All experiments conducted in this study were performed at least in triplicate independently. The statistical analysis was performed by Prism 8 (GraphPad, USA), and data were presented as mean ± standard deviation (SD). For

comparison between two groups, the unpaired two-tailed Student's t- test was performed. Ordinary one-way ANOVA (Tukey's multiple comparisons tests) wasperformed for multiple comparisons. A value of $P < .05$ was considered to be statistically significant.

Results

Single-Cell Transcriptional Profiling Identifies a Subcluster of Late RPCs Associated With Photoreceptor Differentiation

To investigate the temporal transcriptional profiling during retinal development, we performed single-cell RNA sequencing (scRNA-seq) analysis of 6 retinas obtained from embryos or early-born mice. Each time point contained 2 retinas, including E14, E17, and P3, which corresponded to the early, late embryonic, and postnatal stages of retinal development (Supplementary Fig. S1A).[22] The samples were comparable in terms of number of cells and genes per cell analyzed (Supplementary Fig. S1A).

To classify cell types in the developing mouse retina, we performed a uniform manifold approximation and projection (UMAP)[23] analysis and identified 7 major clusters, including early RPCs (RPC-1), late RPCs (RPC-2), ciliary margin zone (CMZ) cells, retinal ganglion cells (RGCs), photoreceptors (PRs), amacrine cells and horizontal cells (AC/HC), and early Müller glia (MG) (Fig. 1A). Each individual cell was annotated based on the transcriptional patterns of transcripts enriched within particular clusters (Supplementary Fig. S1B). Clusters predominantly matched each sampled time point when visualized using UMAP analysis (Fig. 1B). A pseudotemporal analysis was performed on subsets of specific cell types. It uncovered that the late RPCs subset connected between early RPCs and mature retinal cell types, including RGCs, PRs, and AC/HC, suggesting late RPCs might differentiate into RGCs, PRs, and AC/HC (Fig. 1C). Compared with RPC-2, more cell proliferation related-genes such as *Ccnd1*, *Nr2e1*, and *Fgf9* were activated in RPC-1 (Supplementary Fig. S1C). Multiple neurogenic bHLH factors, such as *Atoh7*, *Olig2*, and *Neurog2*, Notch-ligand Delta-like gene family *Dll1* and cell cycle exiting gene *Top2a* were expressed by RPC-2, indicating that the cluster of late RPCs went through terminal dividing, consistent with previous reports that bHLH genes are expressed in cell cycle-exiting RPCs (Fig. 1D, Supplementary Fig. S1C).[24,25] According to GO function enrichment analysis, the high expression genes enriched in RPC-2 were related to cell differentiation while those in RPC-1 were important for cell proliferation and development (Supplementary Fig. S1D). The top 20 genes expressed in this cluster were listed in Fig. 1E, including bHLH genes and Notch signaling components *Dll1*, *Dll3*, *Dll4*, *Hes5*, and *Hes6*. The late RPCs cluster was subdivided into 3 discrete clusters by the 2D *t*-stochastic neighbor embedding (tSNE) analysis (C1-C3) distinguished by differential gene expression associated with competence transitions, regulation of neurogenic divisions, and cell fate specification (Fig. 1F). There was no significant difference in temporal distribution among the 3 subclusters. In contrast, C1 cells were more mitotically active than C2 and C3, as C2 and C3 cells gradually exited the cell cycle. Upon analyzing the heterogeneity of gene expressions, we noticed that C1 cells exhibited high expression levels of genes involved in regulating cell proliferation and mitosis, such as *Ccnd1*,[26] *Itm2a*,[27] *Fgf15*,[28] *Dapl1*[29], and *Hes1*,[30] as well as cell division, including *Mcm6*,[31] *Pcna*[32], and *Lig2*.[33] Intriguingly, C2 cells were more likely to be transcriptionally related to photoreceptor differentiation, including *Otx2*,[34] *Olig2*,[25] and *Dll4*.[35] Other genes such as *Pcdh17*,[36] *Meg3*,[37] *Igsf21*,[38] and *Pkib*,[39] which are mainly involved in synaptic development and neurotransmitter transport, were also expressed at high levels in C2. Of note, C3 cells showed a correlation with ganglion cell components due to their high expression of *Atoh7*,[40] *Dlx1*, *Dlx2*[41], and *Tubb3*.[42] In addition, development and differentiation-related genes, including *Gal*,[43] *Phlda1*,[44] *Insm2*[45,46], and *Ppp1r14b*,[47] were highly expressed in C3 (Fig. 1G). Based on the scRNA-seq analysis, we demonstrated the transcriptome profiling of late RPCs subpopulation and identified a subcluster of late RPCs associated with photoreceptor differentiation.

Surface Protein Sstr2 Is Highly Expressed in Late RPCs During Mouse Retinal Development

To compare the surface marker profiles between early RPCs and late RPCs, we analyzed the surface proteins highly expressed in RPC-1 and RPC-2. It showed that *Slc3a2* (*CD98*) and *Cxcr4* (*CD184*) were highly expressed in the early RPCs group (RPC-1) (Fig. 2A), while *Itga6* (*CD49f*) and *Itgb1* (*CD29*) were expressed in both early RPCs and late RPCs. Notably, *Sstr2*, one of the somatostatin receptors, was highly expressed in late RPCs (RPC-2), consistent with a previous report that *Sstr2* was involved in retinal neurogenesis.[48] In line with expression levels, UMAP analysis revealed that *Sstr2* was mainly expressed in the RPC-2 cluster (Fig. 2A). Since the RPC-2 cluster was divided into subclusters (C1, C2, and C3) (Fig. 1F), the gene expression of *Sstr2* in different subclusters was further analyzed. *Sstr2* was highly expressed in subcluster C2 (Fig. 1G) and was mainly colocalized with *Olig2* and *Neurog2*, which were related to photoreceptor differentiation in the C2 subcluster (Fig. 2B). This indicates that Sstr2 may be a potential marker for screening the late RPCs subgroup for stem cell therapy. To investigate the feasibility and optimal timing of enriching $Sstr2^+$ cells from the developing mouse retina, we further investigated the temporal and spatial distribution of Sstr2 expression during the developmental mouse retina. Violin plots demonstrated a high expression level of Sstr2 in E17, followed by a decrease at P3 in both retinal and RPC-2 cells (Fig. 2C and D). An immunofluorescent assay was carried out to detect the spatial distribution and cell morphology of $Sstr2^+$ cells. Consistent with scRNA-seq data, the protein expression of Sstr2 was transiently higher in the embryonic stage but was gradually diminished in the postnatal stage (Fig. 2C and 2E). Similarly, the number of cells expressing Sstr2 increased in the embryonic stage, peaked at around E17, and gradually decreased at the postnatal stage. During the early stage of retinal neurogenesis, Sstr2 was mainly expressed in the neural retina (NR) at E12-E14. At this time, $Sstr2^+$ cells coexpressed with RPC markers such as Olig2, Otx2, and Sox2 (Fig. 2E). At the intermediate stage of retinal neurogenesis, Sstr2 was expressed mainly in the outer neuroblastic layer (ONBL) at E17 and P0, where RPCs and photoreceptor precursors reside, and partially overlapped with Olig2, Otx2, and Sox2. At the late stage of retinal neurogenesis, $Sstr2^+$ cells were in the inner neuroblastic layer (INBL) at P3 retina, and mainly in the

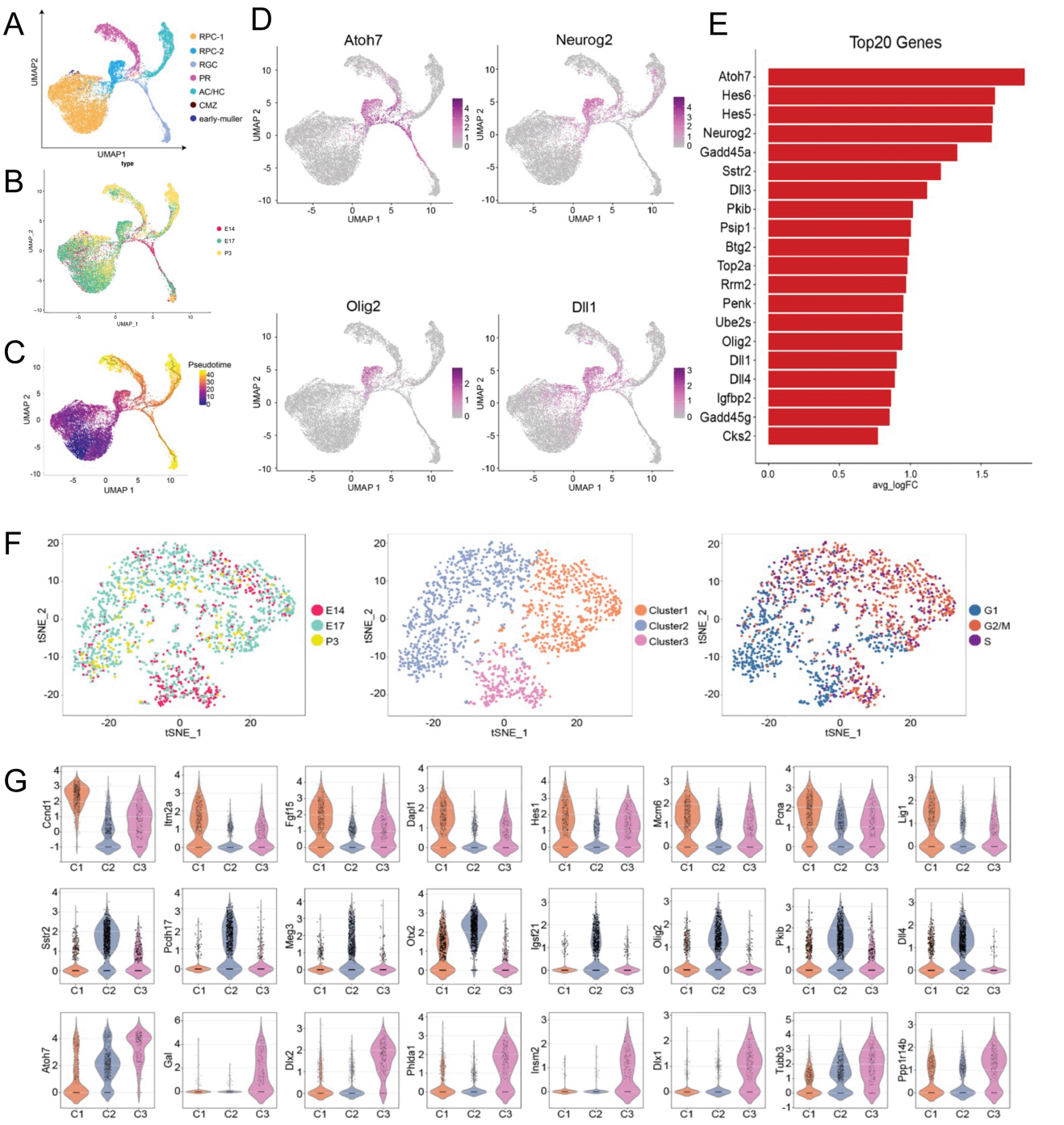

Figure 1. Single-cell RNA sequencing (scRNA-seq) transcriptome profiles of mouse developing retina. (**A**) Cell clusters of cell identity in retinas from E14, E17, and P3 by UMAP. (**B**) UMAP visualization of all mice retinal cells from each time point profiled, with individual cells colored by age. (**C**) Pseudotime analysis of retinal cells from all 3 time points by Monocle3. (**D**) UMAP visualization showing late RPC (RPC-2) at all developmental stages tested specifically expressing bHLH genes (Atoh7, Neurog2, and Olig2) and Notch signaling component (Dll1). (**E**) Top 20 genes expressing in RPC-2 cluster compared with other clusters. (**F**) tSNE analysis showing subclusters of RPC-2 among 3 time points and their cell cycle status. (**G**) Violin plot showing differentially expressed genes between three subclusters of RPC-2. Abbreviations: RPC: retinal progenitor cells; RGC: retinal ganglion cells; PR: photoreceptors; AC/HC: amacrine cells/horizontal cells; CMZ: ciliary margin zone.

inner retinal layer at P7 retina. Interestingly, Sstr2 protein was not detected in the ciliary margin at E12 to E14. But a proportion of Sstr2$^+$ cells were detected in the ciliary margin starting from E17 to P3 (Fig. 2E). Collectively, we identified a surface marker Sstr2 distinctly expressed in late RPCs and revealed its spatiotemporal expression pattern during mouse retinal development.

Sstr2$^+$ Cells in the Late Embryonic Retina Commit Toward Cones, Amacrine and Horizontal Cells During Retinal Development

Previous studies have reported that Sstr2 was expressed in neurogenic and photoreceptor-competent RPCs.[48] But how Sstr2$^+$ neurogenic RPCs determine their cell fate remains largely elusive. As such, we employed the Cre-loxP

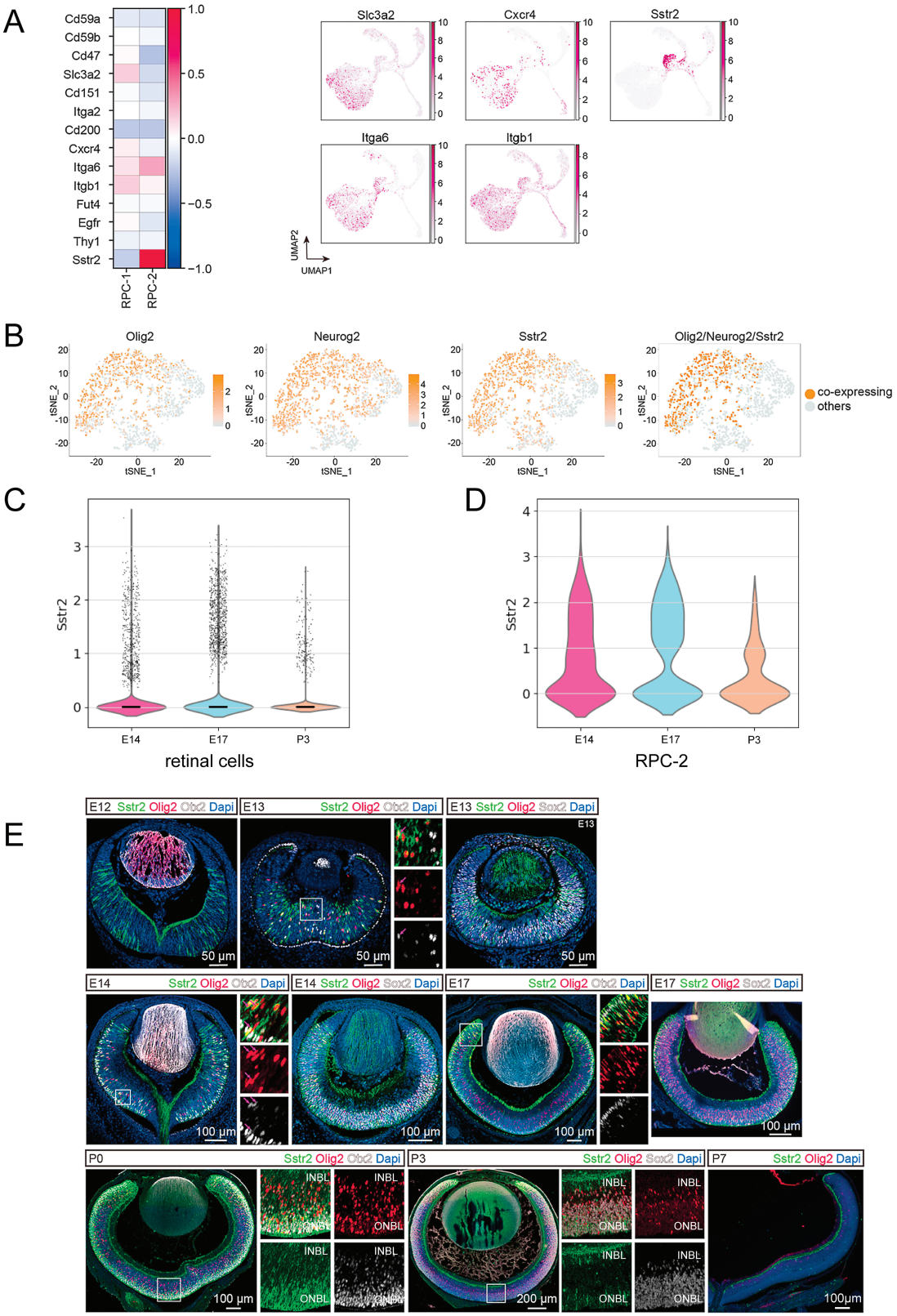

Figure 2. Surface protein Sstr2 is highly expressed in late RPCs during mouse retinal development. (**A**) Heatmap showing Sstr2 and other surface markers expression in RPC-1 and 2 cells. (**B**) Expression of bHLH Genes (Olig2 and Neurog2) and Sstr2 within the tSNE plots of all RPC-2 cells. (**C-D**) Violin plots showing the expression of Sstr2 at different development time points in retinal cells and RPC-2 cells. (**E**) immunofluorescence detection of Sstr2, Olig2, Otx2, and Sox2 in retina slices from E12, E13, E14, E17, P0, P3, and P7 mice. Abbreviations: INBL: inner neuroblastic layer; ONBL: outer neuroblastic layer.

recombination system controlled by tamoxifen for in vivo genetic lineage tracing to map the differentiation trajectory of Sstr2$^+$ stem cells.[49] We bred the *Sstr2$^{CreERT2+}$mCherry* transgenic mouse using the Cre-loxP system to track the developmental trajectory of Sstr2$^+$ RPCs at the late embryonic stage (E16-E18). At this time, the late RPCs are still mitotic and undergo cell division.[22] After one time in utero exposure of tamoxifen on E16, eye samples were collected on E18, P7, P14, and P28 (Fig. 3A). Immunofluorescence was carried out to explore how Sstr2-mCherry$^+$ lineage cells relate to RPCs or photoreceptor precursor cells by staining RPC markers Olig2 and Otx2 and the photoreceptor precursor cells marker Crx.[25,50,51] In the E18 mouse retina, mCherry$^+$ cells were distributed in inner and outer nuclear layers (INL and ONL), with some cells coexpressing Olig2 (Fig. 3B). In particular, most mCherry$^+$ cells in the ONL expressed Otx2 or Crx (Fig. 3B). In P7, mCherry$^+$ cells were mainly in the inner part of INL and the outer part of ONL (Fig. 3C). Very few mCherry$^+$ cells expressed Olig2 and Otx2, and some mCherry$^+$ cells in ONL expressed Crx (Fig. 3C). By P14 when retinal neurogenesis is completed, mCherry$^+$ cells were scattered in the outer part of ONL, INL, and ganglion cell layer (GCL) without counterstaining with Olig2, Otx2 or Crx (Fig. 3D and 3E).

The mCherry-labeled retina sections from P14 mice displayed the distribution pattern of mCherry$^+$ cells across the ONL, INL, and GCL layers (Fig. 4A). To determine the specific retinal cell types originating from mCherry$^+$ cells, mature retinal cell markers were costained with mCherry. At P14, costaining the pan-cone marker Arrestin with mCherry confirmed the differentiation of mCherry$^+$ cells into cones, although not all cones in the ONL were positive for mCherry (Fig. 4B). Subsequently, colabeling mCherry with cone subtype markers M/L-opsin and S-opsin revealed that mCherry$^+$ cells expressed these markers, indicating differentiation into cone subtypes (Fig. 4C and 4D). Notably, mCherry$^+$ cells did not differentiate into rod cells, as there was no colocalization with the rod marker Rhodopsin (Fig. 4H). We also examined inner neuron markers and observed some mCherry$^+$ cells colocalized with the horizontal cell marker Calbindin, as well as the amacrine cell markers AP2α and Calretinin, indicating differentiation into horizontal and amacrine cells (Fig. 4E-4G). Furthermore, there was no colocalization observed between mCherry and other retinal cell markers, including bipolar cells (PKCα), Müller cells (Vimentin), and retinal ganglion cells (Brn3) (Fig. 4I-4K). Similarly, in adult mouse retinas (P28), mCherry$^+$ cells were colocalized with pan-cone marker Arrestin, horizontal cell marker Calbindin, and amacrine cell markers AP2α and Calretinin (Supplementary Fig. S2A-S2D), but not with other retinal cell markers (Supplementary Fig. S2E-S2H). In summary, our in vivo genetic lineage tracing indicated that Sstr2$^+$ cells in the late embryonic retina differentiate into cone, amacrine, and horizontal cells during retinal development. These findings suggest that Sstr2 could serve as a potential marker for enriching cone-competent RPCs at a relatively high level.

Sstr2$^+$ Cells Isolated From E18 Mouse RPCs Are a Subpopulation of Late RPCs That can Differentiate Into Cones In Vitro

To further confirm the feasibility of using surface protein Sstr2 to enrich cone-competent RPCs, we isolated the Sstr2$^+$ cells from the E18 *Sstr2$^{CreERT2+}$mCherry* transgenic mouse retinas (Fig. 5A) and characterized their differentiation ability. Metabolite 4-hydroxy-tamoxifen, the inducer of the recombinant activity of Cre-ERT, was applied to activate the mCherry expression in Sstr2$^+$ RPCs.[52,53] Gradient concentrations of 4-OHT were tested to determine the optimum concentration of 4-OHT to activate mCherry without causing in vitro cytotoxicity determined by terminal deoxynucleotidyl transferase dUTP nick end labeling (TUNEL).[52,54] We found 2 μm 4-OHT treatment for 48 hours on the Sstr2$^+$ RPCs could activate mCherry without compromising cell viability (Supplementary Fig. S3). The isolated Sstr2$^+$ cells and Sstr2$^-$ cells were both partially positive for RPC markers Olig2 and Sox2 and photoreceptor precursor cell marker Otx2 and Crx (Fig. 5B). While the proportions of Sstr2$^+$ cells and Sstr2$^-$ cells expressing the RPC markers Olig2 and Sox2 were comparable, Sstr2$^+$ cells expressed the photoreceptor precursor cell indicators Otx2 and Crx in a larger percentage than Sstr2$^-$ cells. (Fig. 5C). Sstr2$^+$ cells were further cultured in a modified photoreceptor differentiation media[18,55,56] for 2 weeks and detected by immunofluorescence staining (Fig. 5D), and the differentiated cells expressed the pan-cone marker Arrestin and subtype cone markers M/L-opsin and S-opsin, but not the rod marker Rhodopsin (Fig. 5E). Taken together, our data demonstrated that the Sstr2$^+$ cells isolated from E18 mouse RPCs are a subpopulation of late RPCs that can differentiate into cones in vitro.

Sstr2$^+$ RPCs can Differentiate Into Cones but not Rods in Wild-Type Mice and rd10 Mice

To evaluate the in vivo differentiation potential of Sstr2$^+$ cells, we conducted subretinal transplantation of the previously isolated Sstr2$^+$ cells (Fig. 5) into both wild-type and retinal degeneration 10 (rd10) mutant mice at P14. After a 2-week period post-transplantation, the transplanted mCherry-positive Sstr2$^+$ cells were predominantly observed within the subretinal space in both wild-type and rd10 mice (Fig. 6A-H). Notably, these transplanted mCherry-positive cells exhibited coexpression with the pan-cone marker Arrestin (Fig. 6A and 6E), as well as cone subtype markers M/L-opsin and S-opsin (Fig. 6B, 6C, 6F, and 6G). Importantly, there was no colocalization observed between the transplanted cells and the rod marker Rhodopsin (Fig. 6D and 6H). These findings collectively indicate that Sstr2$^+$ RPCs from the late embryonic mouse retina have the capability to differentiate into various cone cell subtypes, while excluding rod cell differentiation, following transplantation into both wild-type and rd10 mice. This discovery offers an innovative approach for enhancing the enrichment of cone-competent RPCs in the context of treating retinal degeneration.

Discussion

Identification of specific cell population through cell sorting provides valuable resources for stem cell therapy of RD. Recently, the lack of surface markers that can effectively screen and enrich progenitors/precursors with efficient cone differentiation potential has emerged as a significant issue. Here, we have identified Sstr2 as a potential surface marker capable of labeling a subpopulation of late RPCs associated with photoreceptor differentiation via scRNA-seq. Through lineage tracing, it revealed that Sstr2$^+$ late RPCs gave rise to

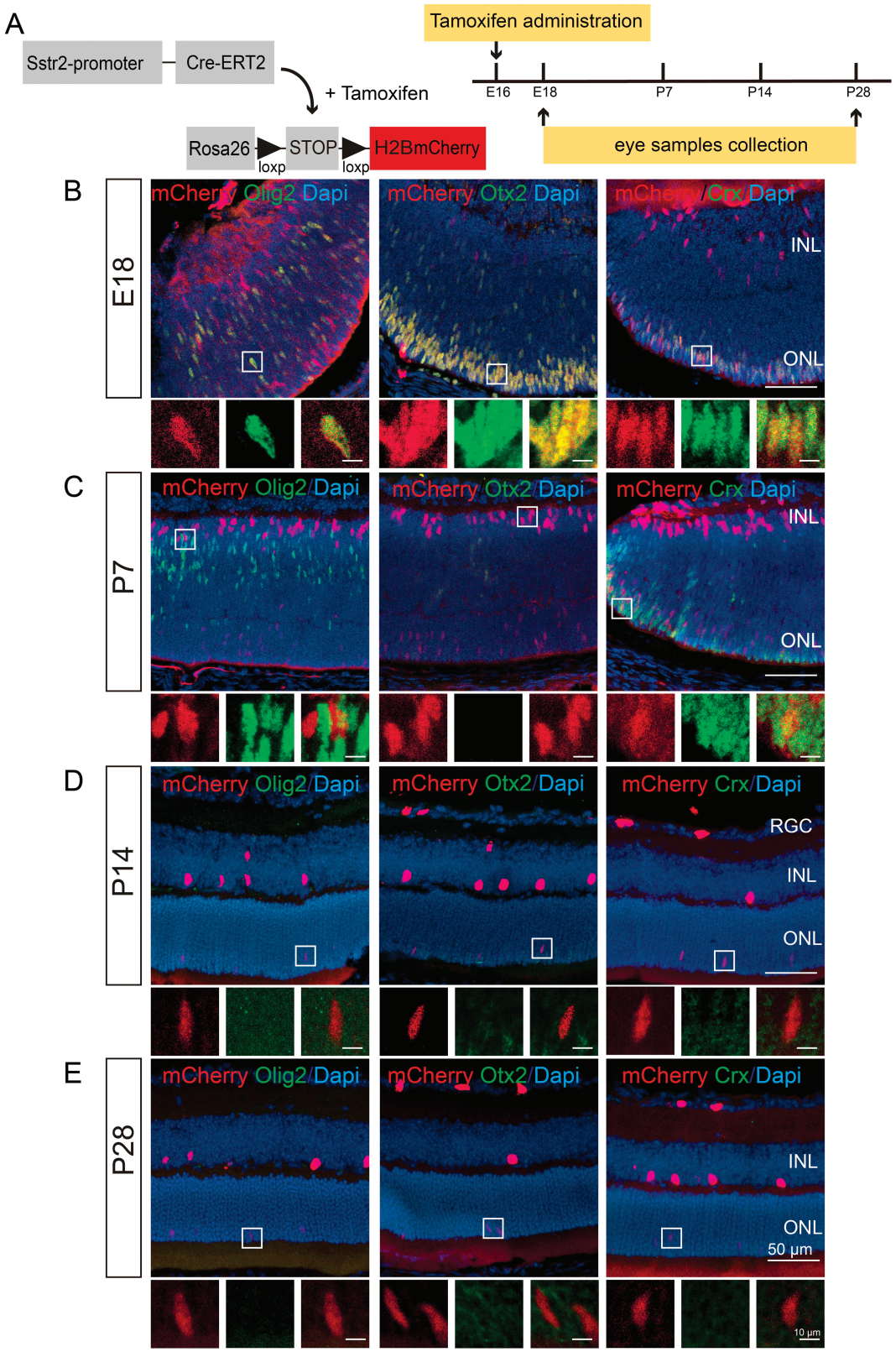

Figure 3. The Sstr2+ cells in the late embryonic retina presents RPC markers during development. (**A**) Schematic overview of the genetic strategy used for the Sstr2-mCherry lineage tracing mice. Diagram for tamoxifen administration and retina collection. Tamoxifen was given on E16, and eye samples were collected on E18, P7, P14, and P28. (**B**-**C**) Immunofluorescence staining showing the colocalization of mCherry+ cells and RPC markers Olig2 and Otx2 or photoreceptor precursor marker Crx on E18 and P7. (**D**-**E**) No colocalization of mCherry+ cells and RPC markers Olig2 and Otx2 or photoreceptor precursor marker Crx was found in P14 and P28 retina. Scale bars = 50 μm (**B**-**D**) and 10 μm (**B**-**D** zoomed box). Abbreviations: RGC: retina ganglion cell; INL: inner nuclear layer; ONL: outer nuclear layer.

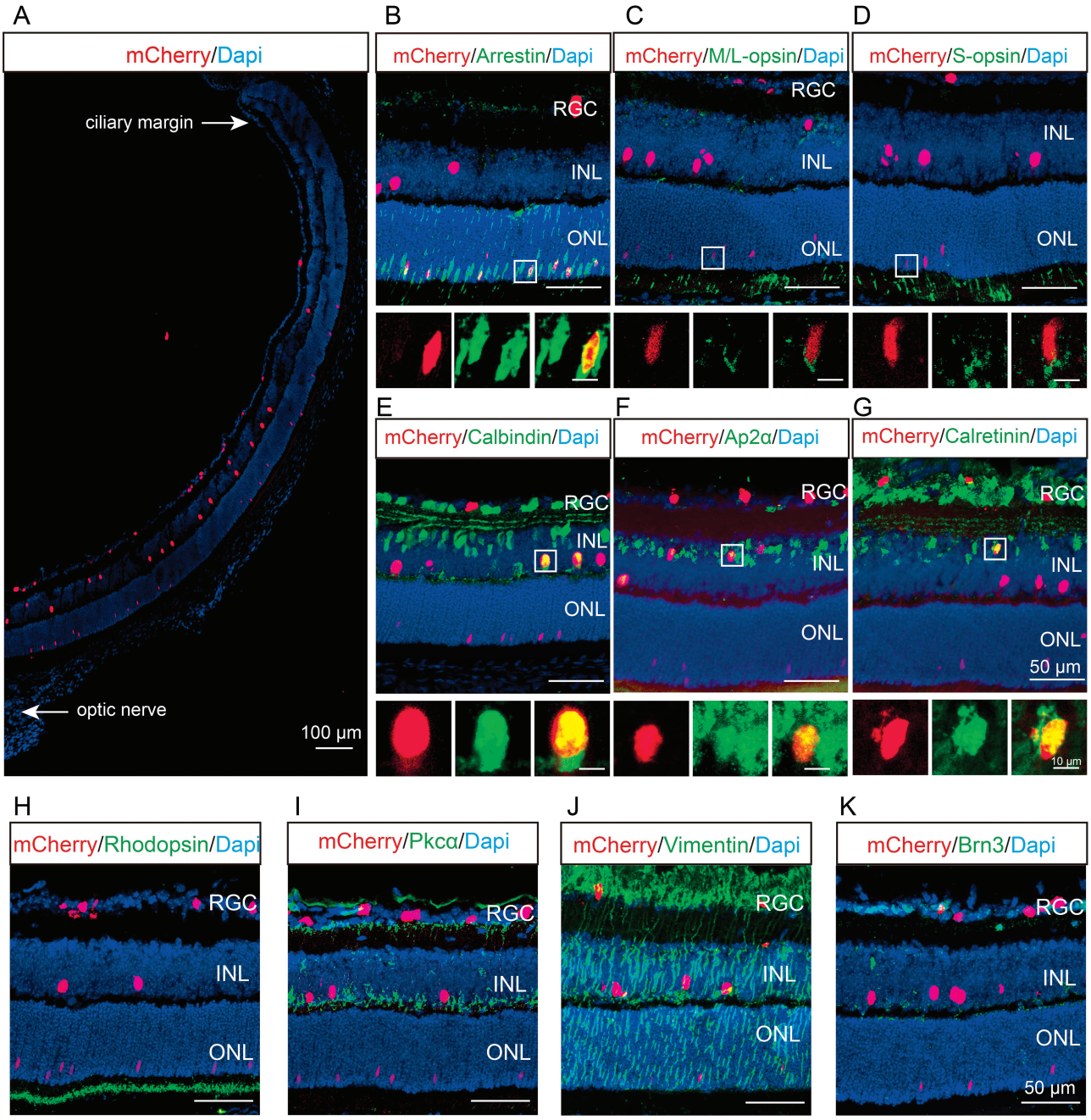

Figure 4. Sstr2+ cells in the late embryonic retina commit toward cone, amacrine, and horizontal cells on P14 Sstr2CreERT2+ mCherry mouse retina. (**A**) Representative image of P14 mouse retina showing the distribution of mCherry+ cells. (**B**-**D**) mCherry+ cells expressed cone makers including Arrestin, M/L-opsin, and S-opsin detected by immunofluorescence staining on P14 retina. (**E**) mCherry+ cells expressed horizontal cell marker Calbindin on P14 retina. (**F**-**G**) mCherry+ cells expressed amacrine cell makers including Ap2α and Calretinin on P14 retina. (**H**) No expression of rod marker Rhodopsin in mCherry+ cells. (**I**-**K**) Brn3 (I), Pkcα (J) and Vimentin (K) were not expressed in mCherry+ cells. Scale bars = 100 μm (A), 50 μm (B-G), and 10 μm (B-G zoomed box), 50 μm (H-K). Abbreviations: RGC: retina ganglion cell; INL: inner nuclear layer; ONL: outer nuclear layer.

cones, amacrine cells, and horizontal cells in adult retina. Furthermore, isolated Sstr2$^+$ late RPCs could express the RPC markers and possess the ability to differentiate into cones in vitro as well as after subretinal transplantation into both WT mice and rd10 mice. This study provides a novel surface marker candidate for isolating late RPCs via scRNA seq, and opens a new perspective for establishing an accurate and efficient cell sorting strategy for treating RD.

Several strategies have been explored to isolate cell source for treating RD. One commonly used approach involves the use of fluorescent protein reporters for particular genes to trace and identify specific cell populations. For instance, donor cells from retinal tissues labeled with the photoreceptor-specific gene Crx, the cone marker Arrestin, or the rod marker Nrl, were stably produced and effectively integrated into the host retina after transplantation.[5,6,57,58] However, the fluorescent protein reporter with gene manipulation may be risky and undesirable for clinical application. FACS via surface markers is an alternative approach for isolating specific cell populations without damage. Cell surface

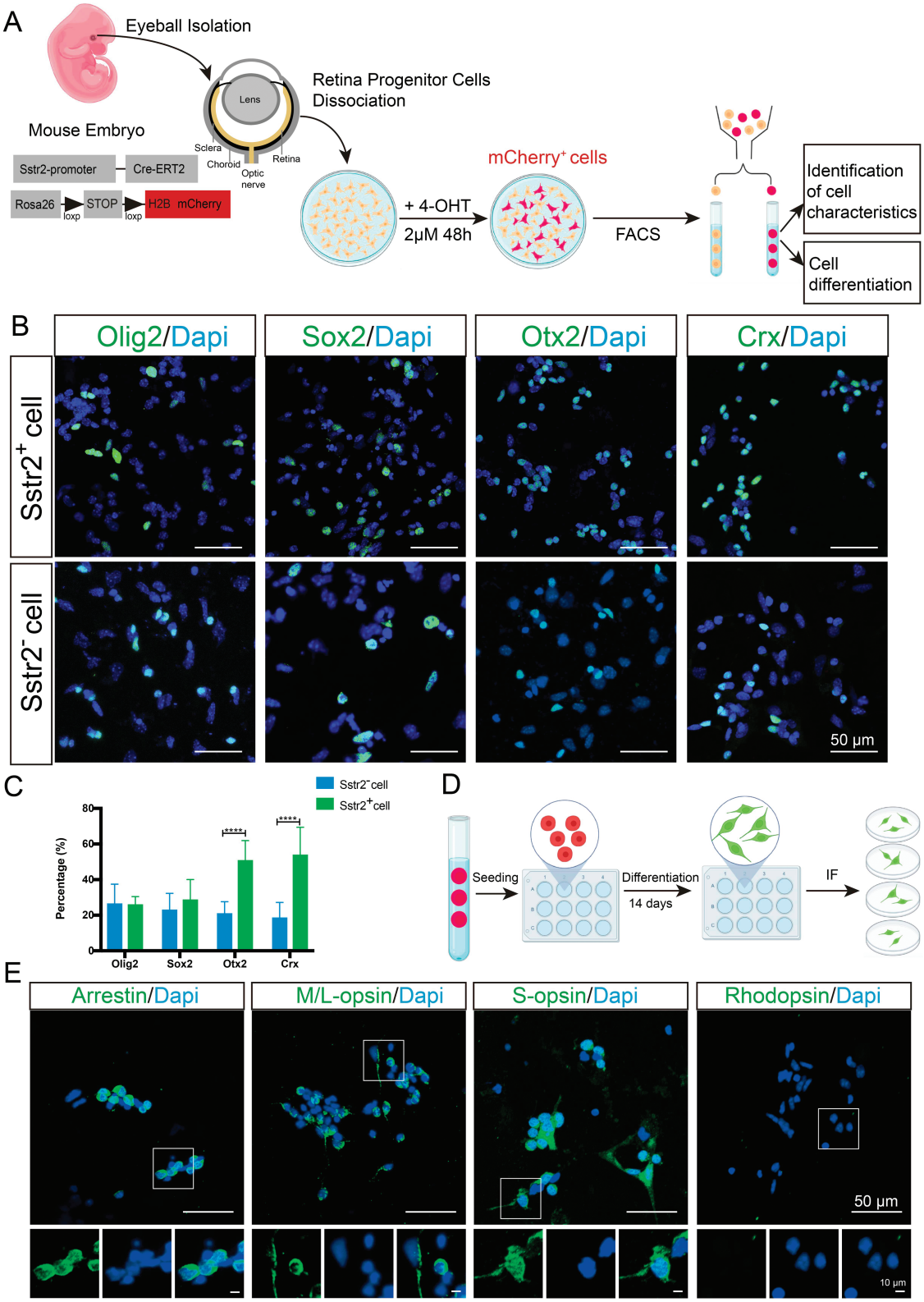

Figure 5. Sstr2+ cells isolated from E18 mouse RPCs are a subpopulation of late RPCs that can differentiate into cones in vitro. (**A**) Schematics for 4-OHT administration to activate the expression of Sstr2 and the identification of Sstr2+ cells in vitro. (**B**) Immunostaining for expression of RPC markers Olig2 and Sox2 and photoreceptor precursor markers Otx2 and Crx in sorted Sstr2+ cells and Sstr2− cells. (**C**) Statistical analysis demonstrating the proportion of Olig2, Sox2, Otx2, and Crx expression in Sstr2+ cells and Sstr2− cells(****$P < .0001$). (**D**) Diagram for Sstr2+ cells differentiation culture. (**E**) The retinal differentiation of sorted Sstr2+ cells into photoreceptors was shown by immunostaining for Arrestin, M/L-opsin, S-opsin, and Rhodopsin. Scale bars = 50 μm (B), 50 μm (E), and 10 μm (E zoomed box). Abbreviations: IF: immunofluorescence.

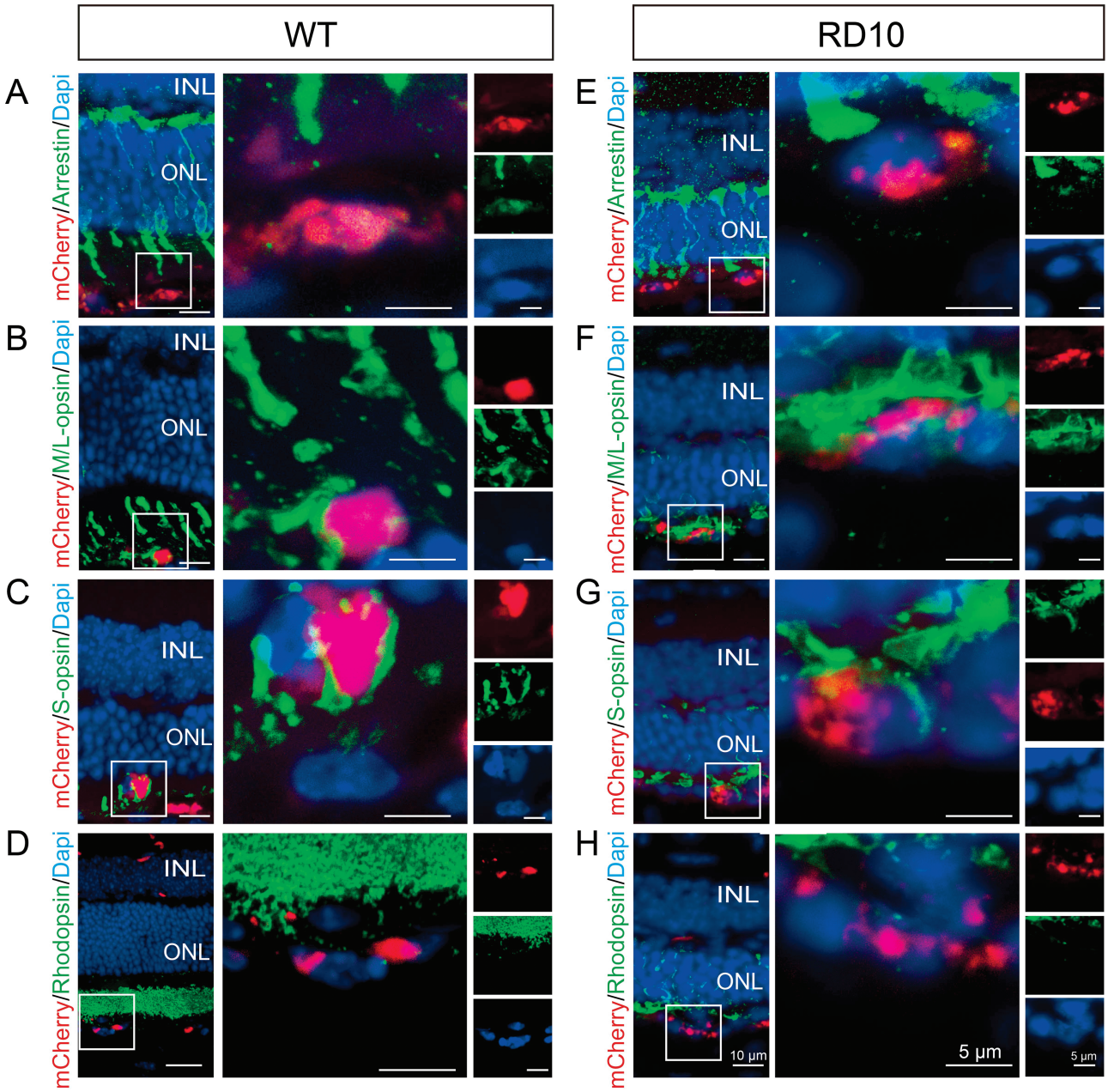

Figure 6. Sstr2+ RPCs can differentiate into cones but not rods in wild-type mice and rd10 mice. (**A**-**C**) Subretinal cell masses of transplanted Sstr2+ cells. Immunostaining for cone marker Arrestin (**A**), cone visual pigments M/L-opsin (**B**), and S-opsin (**C**) of WT mice retina slices. (**D**) Rhodopsin expression was not observed in the transplanted Sstr2+ cells in WT mouse subretinal space. (**E**-**G**) In rd10 mice, retina slices immunostaining showing that Sstr2+ cells overlied with cone marker Arrestin (E), cone-specific phototransduction-related proteins M/L-opsin (F) and S-opsin (G). (**H**) No colocalization of Sstr2+ cells and Rhodopsin was observed by immunofluorescence staining after transplanted into rd10 mice through subretinal injection. Scale bars = 10 μm (A-H), 5μm, and 5μm (A-H zoomed box). Abbreviations: RGC: retina ganglion cell; INL: inner nuclear layer; ONL: outer nuclear layer.

markers have been widely employed in hematology to identify and purify subsets of blood cells, such as hematopoietic stem cells.[59] Some efforts have been made to develop surface markers to screen donor cells from retinal tissue. The previously reported surface markers such as c-Kit, CD73 and combination of $SSEA1^{-}CD133^{+}CD26^{+}CD147^{+}$ were capable of enriching designed retinal cell populations, but not ideal sorting indicators for enriching cones or cone precursors, due to their low specificity for cone cell labeling or low cell sorting rate.[12,15,17,18] Therefore, it is important to find surface markers that can label and enrich cones or cone precursors for cell therapy in retinal degenerative diseases. In addition, the commercially available CD antibodies are not competent, leading to the omission of some potential markers. Therefore, bulk RNA sequencing may provide novel insights for screening surface markers. For example, an Rcvrn-eGFP reporter hiPSCs line combined with bulk RNA sequencing has been utilized to select CD biomarkers for positive selection of rod and cone photoreceptors.[16] While several CD biomarkers highly expressed in RCVRN-eGFP photoreceptors had been identified, the sorting specificity and sensitivity need to be confirmed. Notably, RPCs or photoreceptor precursor cells

of different developmental stages are under dynamic changes with high heterogeneity. However, bulk RNA sequencing provides an average measure of gene expression across all cells in a sample and does not capture individual cell characteristics. Therefore, it does not allow researchers to distinguish between different subpopulations of cells with distinct gene expression profiles. To address this limitation, scRNA-seq techniques are typically required. ScRNA-seq enables the measurement of gene expression in individual cells, thereby facilitating the identification of different subpopulations based on their unique gene expression profiles.[60] Previous studies demonstrated that RPCs were a highly heterogeneous group with significant transcriptional diversities in the early and late stages.[22] Consistently, we found that early and late RPCs were distinct subpopulations. Nevertheless, the late RPCs were still a mixture of cells with varying differentiation capacities into ganglion cells and photoreceptors including cones and rods. Through the application of scRNA-seq, we have unveiled the distinguished Sstr2 as a potential surface marker, which can label a select subpopulation of late RPCs intricately linked to the process of photoreceptor differentiation. Astonishingly, lineage tracing results revealed Sstr2$^+$ late RPCs gave rise to cone cells, amacrine and horizontal cells. In light of this remarkable revelation, Sstr2 emerges as a potential surface marker candidate for relative enrichment of RPCs with a propensity for cone cell differentiation.

As regards retinogenesis, tremendous efforts have been made to identify the factors that regulate retinogenesis. Several scRNA-seq studies had identified some transcription factors specifically expressed on mouse retina's early and late RPCs.[22,61] This study profiled the specified RPCs expressing marker genes of different competencies and bHLH genes, such as *Atoh7*, achaete-scute complex homolog 1 (*Ascl1*), *Neurog2*, and *Olig2*, which were predisposed to generate specific cell subtypes.[24,25,40,62] *Atoh7*, which controls early RGC specification, was selectively expressed in the late RPCs.[24] Although the transient expression of *Atoh7* in postmitotic cells has been well described, the emergence of cells expressing this gene as a distinct cluster was new and helped us to identify other genes that co-expressed in these cells, such as *Neurog2* and *Olig2*.[24,25,62] In this cluster, cells highly expressed bHLH genes *Atoh7*, *Neurog2*, and *Olig2*, indicating these cells underwent terminal neurogenic divisions. These cells also highly expressed a surface protein Sstr2, which overlapped strongly with the expression of *Olig2* and *Neurog2*. The postmitotic cells are low proliferative (less likely to turn into a tumor) and have high differentiating ability, making them ideal donor cells.[63,64] So Sstr2$^+$ late RPCs are ideal donor cells for cone-replacement therapy.

Sstr2 is a gene that encodes for the somatostatin receptor type 2 protein. This receptor is a G-protein coupled receptor that is activated by the neuropeptide somatostatin. The Sstr2 protein is expressed in various cells including the neurogenic cell, endocrine cells, immune cells, and tumor cells and is involved in the neurotransmitters release, regulation of digestive gland secretion, smooth muscle contraction, and cell proliferation.[65] In the adult retina, Sstr2 is mainly expressed in GABA-amacrine cells, with a small portion expressed in horizontal or bipolar cells. It regulates GABA and TH release.[66] In the retinal development of 5 somatostatin receptors (Sstr1-5), Sstr2 is mainly expressed in photoreceptor precursor cells.[67] In addition, Sstr2 was previously found on neurogenic RPCs and played a critical role in the development and maturation of retinal neurons, especially the differentiation and regulation of photoreceptors.[48,67] Consistently, we found that Sstr2 was distinctly expressed in a subpopulation of late RPCs with cone differentiation competency. In this study, Sstr2$^+$ cells partially gave rise to cone photoreceptors in the late embryonic retina. As a note, increased Sstr2 expression was associated with cone differentiation in human retinal organoids, indicating a potential correlation between Sstr2 expression and cone differentiation.[67] However, how Sstr2 affect cone differentiation needs to be clarified. In our study, we analyzed the expression pattern of Sstr2 in the developing mouse retina and found Sstr2 expression at E12 to P3, consistent with Weir et al's report that Sstr2 coincided with its ligand Somatostatin which was abundantly expressed in immature RGCs from E12 to P0.[48] Interestingly, Sstr2$^+$ cells were mainly distributed in the outer retinal layer before birth, where RPCs and photoreceptors are mainly distributed, yet appeared in the inner retina after birth. The observation suggests that Sstr2 affects the development and differentiation of photoreceptor cells. Sstr2 is only detected in the ciliary margin during E17-P3, colocalized with RPC marker Olig2. It is worth noting that retinal neurogenesis begins in the central retina and then progresses to the peripheral retina. During this process, the progenitors at the ciliary margin lose their ability to generate neurons at the postnatal stage.[68] Whether Sstr2 expressed in the ciliary margin regulates RPC proliferation and differentiation in this area needs further investigation.

Further studies in human retinal tissues, specifically in the human fetal retina and hiPSCs-derived retinal organoids, will be necessary for advancing clinical translational applications related to stem cell therapy and donor cell sorting strategies. Sstr2 had been reported to specifically label photoreceptor precursor subpopulation in human ESC-derived retinal organoids analyzed by transcriptome and immunofluorescence.[67] This suggests that we can enrich Sstr2$^+$ cells by FACS from retinal organoids for transplantation to study its therapeutic effect and mechanisms. This will be important for advancing clinical translational applications in cone replacement. However, the spatiotemporal characteristic of Sstr2 on hiPSCs-derived retinal organoids and the feasibility of isolating RPCs with cone differentiation competency through the Sstr2 strategy requires further investigation.

Conclusion

To summarize, our study has successfully identified a distinct subset of late-stage RPCs characterized by the Sstr2 surface protein. Through both scRNA-seq analysis and in vivo lineage tracing in a mouse model, we have demonstrated that these Sstr2$^+$ RPCs possess the unique ability to differentiate into cones, amacrine, and horizontal cells. Moreover, the Sstr2$^+$ cells isolated from the late embryonic mouse retina exhibited RPC markers and displayed the capacity to differentiate into cone cells when cultured in vitro. Additionally, after subretinal transplantation into both wild-type and retinal degenerative mice, the transplanted Sstr2$^+$ cells exhibited survival and expression of cone markers. Our findings strongly indicate that Sstr2 serves as a valuable biomarker for identifying late-stage RPCs with the competence to differentiate into cones, making it a promising tool for enriching RPCs at a relatively high level for cone-based therapeutic transplantation.

Funding

This work was supported by the National Natural Science Foundation of China (No. 82271132, 82201224, 82101128), the Top military medical science and technology youth training project (20QNPY027) and the Beijing Hospitals Authority Youth Program under Grant No. QML20230109. The sponsor or funding organization had no role in the design or conduct of this research.

Conflict of interest

The authors declared no potential conflict of interest.

Author Contributions

B.Y.H., C.X., T.Z., and L.Y. contributed to the study design. H.H. and X.C. performed the sample preparation and single-cell RNA sequencing and the bioinformatics analysis. B.Y.H. performed most of the experiments including immunofluorescence staining, flow cytometry, cell culture, and subretinal transplantation. H.H. performed the immunofluorescence staining. R.B.Q. provided animal models for this study. R.J.Y assisted in subretinal space transplantation. B.Y.H., T.Z., and X.C. contributed to data collection and statistical analysis. B.Y.H., C.X., T.Z., and L.Y. contributed to the manuscript writing. All authors read and approved the final manuscript.

Data Availability

All data used in this study are available from the corresponding author upon reasonable request.

Ethical Statement

The study protocol was approved by the Office of Research Ethics Committee at Southwest Hospital (ethics approval number: AMUWE20223994).

Supplementary Material

Supplementary material is available at *Stem Cells Translational Medicine* online.

References

1. Gagliardi G, Ben M'Barek K, Goureau O. Photoreceptor cell replacement in macular degeneration and retinitis pigmentosa: a pluripotent stem cell-based approach. *Prog Retin Eye Res*. 2019;71:1-25. https://doi.org/10.1016/j.preteyeres.2019.03.001
2. van Lookeren Campagne M, LeCouter J, Yaspan BL, Ye W. Mechanisms of age-related macular degeneration and therapeutic opportunities. *J Pathol*. 2014;232(2):151-164. https://doi.org/10.1002/path.4266
3. Zarbin M. Cell-based therapy for degenerative retinal disease. *Trends Mol Med*. 2016;22(2):115-134. https://doi.org/10.1016/j.molmed.2015.12.007
4. Jin ZB, Gao M-L, Deng W-L, et al. Stemming retinal regeneration with pluripotent stem cells. *Prog Retin Eye Res*. 2019;69:38-56. https://doi.org/10.1016/j.preteyeres.2018.11.003
5. Ribeiro J, Procyk CA, West EL, et al. Restoration of visual function in advanced disease after transplantation of purified human pluripotent stem cell-derived cone photoreceptors. *Cell Rep*. 2021;35(3):109022. https://doi.org/10.1016/j.celrep.2021.109022
6. Gasparini SJ, Tessmer K, Reh M, et al. Transplanted human cones incorporate into the retina and function in a murine cone degeneration model. *J Clin Invest*. 2022;132(12):e154619. https://doi.org/10.1172/JCI154619
7. Liu Y, Chen SJ, Li SY, et al. Long-term safety of human retinal progenitor cell transplantation in retinitis pigmentosa patients. *Stem Cell Res Ther*. 2017;8(1):209. https://doi.org/10.1186/s13287-017-0661-8
8. Maeda T, Mandai M, Sugita S, Kime C, Takahashi M. Strategies of pluripotent stem cell-based therapy for retinal degeneration: update and challenges. *Trends Mol Med*. 2022;28(5):388-404. https://doi.org/10.1016/j.molmed.2022.03.001
9. Sommerkamp P, Romero-Mulero MC, Narr A, et al. Mouse multipotent progenitor 5 cells are located at the interphase between hematopoietic stem and progenitor cells. *Blood*. 2021;137(23):3218-3224. https://doi.org/10.1182/blood.2020007876
10. Koso H, Minami C, Tabata Y, et al. CD73, a novel cell surface antigen that characterizes retinal photoreceptor precursor cells. *Invest Ophthalmol Vis Sci*. 2009;50(11):5411-5418. https://doi.org/10.1167/iovs.08-3246
11. Koso H, Satoh S, Watanabe S. c-kit marks late retinal progenitor cells and regulates their differentiation in developing mouse retina. *Dev Biol*. 2007;301(1):141-154. https://doi.org/10.1016/j.ydbio.2006.09.027
12. Lakowski J, Gonzalez-Cordero A, West EL, et al. Transplantation of photoreceptor precursors isolated via a cell surface biomarker panel from embryonic stem cell-derived self-forming retina. *Stem Cells*. 2015;33(8):2469-2482. https://doi.org/10.1002/stem.2051
13. Zhou PY, Peng G-H, Xu H, Yin ZQ. c-Kit(+) cells isolated from human fetal retinas represent a new population of retinal progenitor cells. *J Cell Sci*. 2015;128(11):2169-2178. https://doi.org/10.1242/jcs.169086
14. Zou T, Gao L, Zeng Y, et al. Organoid-derived C-Kit(+)/SSEA4(-) human retinal progenitor cells promote a protective retinal microenvironment during transplantation in rodents. *Nat Commun*. 2019;10(1):1205. https://doi.org/10.1038/s41467-019-08961-0
15. Gagliardi G, Ben M'Barek K, Chaffiol A, et al. Characterization and transplantation of CD73-positive photoreceptors isolated from human iPSC-derived retinal organoids. *Stem Cell Rep*. 2018;11(3):665-680. https://doi.org/10.1016/j.stemcr.2018.07.005
16. Guan Y, Wang Y, Zheng D, et al. Generation of an RCVRN-eGFP reporter hiPSC line by CRISPR/Cas9 to monitor photoreceptor cell development and facilitate the cell enrichment for transplantation. *Front Cell Dev Biol*. 2022;10:870441. https://doi.org/10.3389/fcell.2022.870441
17. Welby E, Lakowski J, Di Foggia V, et al. Isolation and comparative transcriptome analysis of human fetal and iPSC-derived cone photoreceptor cells. *Stem Cell Rep*. 2017;9(6):1898-1915. https://doi.org/10.1016/j.stemcr.2017.10.018
18. Chen X, Chen Z, Li Z, et al. Grafted c-kit(+)/SSEA1(-) eye-wall progenitor cells delay retinal degeneration in mice by regulating neural plasticity and forming new graft-to-host synapses. *Stem Cell Res Ther*. 2016;7(1):191. https://doi.org/10.1186/s13287-016-0451-8
19. Luecken MD, Theis FJ. Current best practices in single-cell RNA-seq analysis: a tutorial. *Mol Syst Biol*. 2019;15(6):e8746. https://doi.org/10.15252/msb.20188746
20. Macosko EZ, Basu A, Satija R, et al. Highly parallel genome-wide expression profiling of individual cells using nanoliter droplets. *Cell*. 2015;161(5):1202-1214. https://doi.org/10.1016/j.cell.2015.05.002
21. Tirosh I, Izar B, Prakadan SM, et al. Dissecting the multicellular ecosystem of metastatic melanoma by single-cell RNA-seq. *Science (New York, N.Y.)* 2016;352(6282):189-196. https://doi.org/10.1126/science.aad0501
22. Clark BS, Stein-O'Brien GL, Shiau F, et al. Single-cell RNA-Seq analysis of retinal development identifies NFI factors as regulating mitotic exit and late-born cell specification.

Neuron. 2019;102(6):1111-1126.e5. https://doi.org/10.1016/j.neuron.2019.04.010
23. Becht E, McInnes L, Healy J, et al. Dimensionality reduction for visualizing single-cell data using UMAP. *Nat Biotechnol*. 2018;37:38-44. https://doi.org/10.1038/nbt.4314
24. Brzezinski JA, Prasov L, Glaser T. Math5 defines the ganglion cell competence state in a subpopulation of retinal progenitor cells exiting the cell cycle. *Dev Biol*. 2012;365(2):395-413. https://doi.org/10.1016/j.ydbio.2012.03.006
25. Hafler BP, Surzenko N, Beier KT, et al. Transcription factor Olig2 defines subpopulations of retinal progenitor cells biased toward specific cell fates. *Proc Natl Acad Sci U S A*. 2012;109(20):7882-7887. https://doi.org/10.1073/pnas.1203138109
26. Qie S, Diehl JA. Cyclin D1, cancer progression, and opportunities in cancer treatment. *J Mol Med (Berlin, Germany)*. 2016;94(12):1313-1326. https://doi.org/10.1007/s00109-016-1475-3
27. Nguyen TM, Shin I-W, Lee TJ, et al. Loss of ITM2A, a novel tumor suppressor of ovarian cancer through G2/M cell cycle arrest, is a poor prognostic factor of epithelial ovarian cancer. *Gynecol Oncol*. 2016;140(3):545-553. https://doi.org/10.1016/j.ygyno.2015.12.006
28. Uriarte I, Latasa MU, Carotti S, et al. Ileal FGF15 contributes to fibrosis-associated hepatocellular carcinoma development. *Int J Cancer*. 2015;136(10):2469-2475. https://doi.org/10.1002/ijc.29287
29. Ma X, Hua J, Zheng G, et al. Regulation of cell proliferation in the retinal pigment epithelium: differential regulation of the death-associated protein like-1 DAPL1 by alternative MITF splice forms. *Pigment Cell Melanoma Res*. 2018;31(3):411-422. https://doi.org/10.1111/pcmr.12676
30. Murata K, Hattori M, Hirai N, et al. Hes1 directly controls cell proliferation through the transcriptional repression of p27Kip1. *Mol Cell Biol*. 2005;25(10):4262-4271. https://doi.org/10.1128/MCB.25.10.4262-4271.2005
31. Zeng T, Guan Y, Li Y-K, et al. The DNA replication regulator MCM6: an emerging cancer biomarker and target. *Clin Chim Acta Int J Clin Chem*. 2021;517:92-98. https://doi.org/10.1016/j.cca.2021.02.005
32. Dietrich DR. Toxicological and pathological applications of proliferating cell nuclear antigen (PCNA), a novel endogenous marker for cell proliferation. *Crit Rev Toxicol*. 1993;23(1):77-109. https://doi.org/10.3109/10408449309104075
33. Ahmad B, Saeed A, Castrosanto MA, et al. Identification of natural marine compounds as potential inhibitors of CDK2 using molecular docking and molecular dynamics simulation approach. *J Biomol Struct Dyn*. 2022;41(17):8506-8516. https://doi.org/10.1080/07391102.2022.2135594
34. Nishida A, Furukawa A, Koike C, et al. Otx2 homeobox gene controls retinal photoreceptor cell fate and pineal gland development. *Nat Neurosci*. 2003;6:1255-1263. https://doi.org/10.1038/nn1155
35. Luo H, Jin K, Xie Z, et al. Forkhead box N4 (Foxn4) activates Dll4-Notch signaling to suppress photoreceptor cell fates of early retinal progenitors. *Proc Natl Acad Sci U S A*. 2012;109(9):E553-E562. https://doi.org/10.1073/pnas.1115767109
36. Hoshina N, Tanimura A, Yamasaki M, et al. Protocadherin 17 regulates presynaptic assembly in topographic corticobasal Ganglia circuits. *Neuron*. 2013;78(5):839-854. https://doi.org/10.1016/j.neuron.2013.03.031
37. Chen G, Qian H-M, Chen J, et al. Whole transcriptome sequencing identifies key circRNAs, lncRNAs, and miRNAs regulating neurogenesis in developing mouse retina. *BMC Genomics*. 2021;22(1):779. https://doi.org/10.1186/s12864-021-08078-z
38. Tanabe Y, Naito Y, Vasuta C, et al. IgSF21 promotes differentiation of inhibitory synapses via binding to neurexin2α. *Nat Commun*. 2017;8(1):408. https://doi.org/10.1038/s41467-017-00333-w
39. Jia HL, Zeng X-Q, Huang F, et al. Integrated microRNA and mRNA sequencing analysis of age-related changes to mouse thymic epithelial cells. *IUBMB Life*. 2018;70(7):678-690. https://doi.org/10.1002/iub.1864
40. Brodie-Kommit J, Clark BS, Shi Q, et al. Atoh7-independent specification of retinal ganglion cell identity. *Sci Adv*. 2021;7(11):eabe4983. https://doi.org/10.1126/sciadv.abe4983
41. de Melo J, Du G, Fonseca M, et al. Dlx1 and Dlx2 function is necessary for terminal differentiation and survival of late-born retinal ganglion cells in the developing mouse retina. *Development (Cambridge, England)*. 2005;132(2):311-322. https://doi.org/10.1242/dev.01560
42. Gudiseva HV, Vrathasha V, He J, et al. Single cell sequencing of induced pluripotent stem cell derived retinal ganglion cells (iPSC-RGC) reveals distinct molecular signatures and RGC subtypes. *Genes*. 18 2021;12(12):2015. https://doi.org/10.3390/genes12122015
43. Cordero-Llana O, Rinaldi F, Brennan PA, Wynick D, Caldwell MA. Galanin promotes neuronal differentiation from neural progenitor cells in vitro and contributes to the generation of new olfactory neurons in the adult mouse brain. *Exp Neurol*. 2014;256:93-104. https://doi.org/10.1016/j.expneurol.2014.04.001
44. Shu L, Du C. PHLDA1 promotes sevoflurane-induced pyroptosis of neuronal cells in developing rats through TRAF6-mediated activation of Rac1. *Neurotoxicology*. 2022;93:140-151. https://doi.org/10.1016/j.neuro.2022.09.007
45. Wang L, Sun ZS, Xiang B, et al. Targeted deletion of Insm2 in mice result in reduced insulin secretion and glucose intolerance. *J Transl Med*. 2018;16(1):297. https://doi.org/10.1186/s12967-018-1665-6
46. Cai T, Chen X, Wang R, et al. Expression of insulinoma-associated 2 (INSM2) in pancreatic islet cells is regulated by the transcription factors Ngn3 and NeuroD1. *Endocrinology*. 2011;152(5):1961-1969. https://doi.org/10.1210/en.2010-1065
47. Lang I, Virk G, Zheng DC, et al. The evolution of duplicated genes of the Cpi-17/Phi-1 (ppp1r14) family of protein phosphatase 1 inhibitors in teleosts. *Int J Mol Sci*. 2020;21(16):5709. https://doi.org/10.3390/ijms21165709
48. Weir K, Kim DW, Blackshaw S. A potential role for somatostatin signaling in regulating retinal neurogenesis. *Sci Rep*. 2021;11(1):10962. https://doi.org/10.1038/s41598-021-90554-3
49. Kretzschmar K, Watt FM. Lineage tracing. *Cell*. 2012;148(1-2):33-45. https://doi.org/10.1016/j.cell.2012.01.002
50. Furukawa T, Morrow EM, Cepko CL. Crx, a novel otx-like homeobox gene, shows photoreceptor-specific expression and regulates photoreceptor differentiation. *Cell*. 1997;91(4):531-541. https://doi.org/10.1016/s0092-8674(00)80439-0
51. Baas D, Bumsted KM, Martinez JA, et al. The subcellular localization of Otx2 is cell-type specific and developmentally regulated in the mouse retina. *Brain Res Mol Brain Res*. 2000;78(1-2):26-37. https://doi.org/10.1016/s0169-328x(00)00060-7
52. Ito SI, Onishi A, Takahashi M. Chemically-induced photoreceptor degeneration and protection in mouse iPSC-derived three-dimensional retinal organoids. *Stem Cell Res*. 2017;24:94-101. https://doi.org/10.1016/j.scr.2017.08.018
53. Fuhrmann-Benzakein E, García-Gabay I, Pepper MS, Vassalli JD, Herrera PL. Inducible and irreversible control of gene expression using a single transgene. *Nucleic Acids Res*. 2000;28(23):E99. https://doi.org/10.1093/nar/28.23.e99
54. Movahedan A, Afsharkhamseh N, Sagha HM, et al. Loss of Notch1 disrupts the barrier repair in the corneal epithelium. *PLoS One*. 2013;8(7):e69113. https://doi.org/10.1371/journal.pone.0069113
55. Osakada F, Ikeda H, Mandai M, et al. Toward the generation of rod and cone photoreceptors from mouse, monkey and human embryonic stem cells. *Nat Biotechnol*. 2008;26(2):215-224. https://doi.org/10.1038/nbt1384
56. Forouzanfar F, Soleimannejad M, Soltani A, Sadat Mirsafaee P, Asgharzade S. Retinoic acid and taurine enhance differentiation of the human bone marrow stem cells into cone photoreceptor cells and retinal ganglion cells. *J Cell Biochem*. 2021;122(12):1915-1924. https://doi.org/10.1002/jcb.30151
57. Lakowski J, Baron M, Bainbridge J, et al. Cone and rod photoreceptor transplantation in models of the childhood retinopathy Leber congenital amaurosis using flow-sorted Crx-positive donor

cells. *Hum Mol Genet*. 2010;19(23):4545-4559. https://doi.org/10.1093/hmg/ddq378
58. Phillips MJ, Capowski EE, Petersen A, et al. Generation of a rod-specific NRL reporter line in human pluripotent stem cells. *Sci Rep*. 2018;8(1):2370. https://doi.org/10.1038/s41598-018-20813-3
59. Haylock DN, Williams B, Johnston HM, et al. Hemopoietic stem cells with higher hemopoietic potential reside at the bone marrow endosteum. *Stem Cells*. 2007;25(4):1062-1069. https://doi.org/10.1634/stemcells.2006-0528
60. Stuart T, Satija R. Integrative single-cell analysis. *Nat Rev Genet*. 2019;20(5):257-272. https://doi.org/10.1038/s41576-019-0093-7
61. Lyu P, Hoang T, Santiago CP, et al. Gene regulatory networks controlling temporal patterning, neurogenesis, and cell-fate specification in mammalian retina. *Cell Rep*. 2021;37(7):109994. https://doi.org/10.1016/j.celrep.2021.109994
62. Brzezinski JA, Kim EJ, Johnson JE, Reh TA. Ascl1 expression defines a subpopulation of lineage-restricted progenitors in the mammalian retina. *Development (Cambridge, England)*. 2011;138(16):3519-3531. https://doi.org/10.1242/dev.064006
63. MacLaren RE, Pearson RA, MacNeil A, et al. Retinal repair by transplantation of photoreceptor precursors. *Nature*. 2006;444(7116):203-207. https://doi.org/10.1038/nature05161
64. Pearson RA, Barber AC, Rizzi M, et al. Restoration of vision after transplantation of photoreceptors. *Nature*. 2012;485(7396):99-103. https://doi.org/10.1038/nature10997
65. Maubert E, Slama A, Ciofi P, et al. Developmental patterns of somatostatin-receptors and somatostatin-immunoreactivity during early neurogenesis in the rat. *Neuroscience*. 1994;62(1):317-325. https://doi.org/10.1016/0306-4522(94)90335-2
66. Thermos K. Functional mapping of somatostatin receptors in the retina: a review. *Vis Res*. 2003;43(17):1805-1815. https://doi.org/10.1016/s0042-6989(03)00169-x
67. Chen M, Mao X, Huang D, et al. Somatostatin signalling promotes the differentiation of rod photoreceptors in human pluripotent stem cell-derived retinal organoid. *Cell Prolif*. 2022;55(7):e13254. https://doi.org/10.1111/cpr.13254
68. Murcia-Belmonte V, Erskine L. Wiring the binocular visual pathways. *Int J Mol Sci*. 2019;20(13):3282. https://doi.org/10.3390/ijms20133282